eXPRESS Polymer Letters Vol.15, No.12 (2021) 1126–1134
Available online at www.expresspolymlett.com
https://doi.org/10.3144/expresspolymlett.2021.91

Epoxy acrylate-based shape memory polymer via 3D printing

W. Shan[1,2], H. Zhong[1], H. Mo[1], S. Zhao[1], P. Liu[3]*

[1]Hunan Electrical College of Technology, 411201 Xiangtan, PR China
[2]College of Mechanical and Vehicle Engineering, Hunan University, 410012 Changsha, PR China
[3]School of Mechanical and Electrical Engineering, Guilin University of Electronic Technology, 541004 Guilin, PR China

Received 1 April 2021; accepted in revised form 17 July 2021

Abstract. Epoxy acrylate (EA) resin, due to its thermo-mechanical properties, performs excellent shaper memory properties. 3D printing opens new opportunities to fabricated shape memory polymer (SMP), which contributed to a rising variety of applications, also requires 3D-printable capability with more advanced shape-memory function and mechanical performance of the material. In this paper, a new strategy was developed to fabricate high strain EA-based SMP through digital light processing (DLP) 3D printing, which took advantage of free radical copolymerization of epoxy acrylate-based oligomer and monomers. The 3D-printed SMP showed high strain at break (up to 90%), thermal stability, as well as excellent shape memory performance. In addition, the shape memory-based self-driven electronics was fabricated by combining shape memory polymer with light-absorbing and conductive ink. The device could change its configuration in response to light and temperature, which has great potential application for soft robotics, flexible electronics, and intelligent control devices.

Keywords: *smart polymers, epoxy acrylate resin, 3D printing, shape memory polymer, self-driven electronics*

1. Introduction

Thermo-responsive SMPs, which are functional materials, could recover their shape in response to temperature. Many polymers, which proved shape memory properties having a large strain at break, but low shape recovery efficiency [1, 2]. Besides good thermal-mechanical properties, EA-based SMP exhibits excellent shape memory properties [3, 4]. Thanks to the development of 3D printing, EA-based SMP has a vast potential application in soft robots, flexible electric devices, and medical, *etc*. However, EA-based SMPs generally have a limit strain at break [5, 6], resulting in low shape memory cycles. Hence, a high strain EA-based SMP has to be developed.

3D printing technology, known as additive manufacturing (AM) or rapid prototyping, layered manufacturing, solid freeform fabrication technology, refers to ways to fabricate 3D objects through a layer-by-layer process [7]. 3D printing technology enables faster turnaround on the design and manufacturing of customized 3D objects tailored to meet the demands of individuals and specific applications, which is gaining popularity in different research fields and has shown considerable progress in recent years [8]. Primarily, 3D printing technology is becoming widespread in the fields of physical models [9, 10], tissue engineering [11, 12], electronic devices [13, 14], as well as microfluidics [15, 16]. Until now, several 3D printing techniques have been developed, including fused deposition modeling (FDM), fused filament fabrication (FFF), and stereolithography (SLA), digital light processing (DLP), powder bed fusion (SLS), material and binder jetting (inkjet and aerosol 3D printing), *etc*. [8, 17, 18]. Among them, digital light processing (DLP) printing is a top-down 3D printing method that has several advantages over other 3D

*Corresponding author, e-mail: hao122012@163.com

printing systems, including shorter curing time, high resolution, smaller volume of resin required during printing, as well as customized and more selective material for 3D printing [7, 8, 17].

Recently, digital light processing (DLP) printing was applied to fabricate functional materials, including hydrogels [19, 20], SMP [21–23], as well as elastomers [24, 25]. These materials could change the configuration when responding to environmental stimuli, including heat, light, and water [26]. Thus, the utilization of stimuli-responsive materials fabricated by digital light processing (DLP) printing contributed to a rising variety of applications of 3D printing, including actuators [20, 21, 27], soft robots [26, 28], and flexible electronics [25, 29].

Wang *et al*. [30] developed a UV-curable epoxy by cross-linking 3-ethyl-3-oxetanemethanol (TMPO) and diglycidyl ether of bisphenol F (DGEBF) with shape memory performance and improved toughness and provides the epoxy system for 3D-printable shape-memory materials. In addition, Peng *et al*. [21] developed the copolymerization of acrylic monomers and an ion-pair comonomer, and successfully 3D printed with a digital light processing (DLP) printer, they demonstrated shape memory microfluidics as a proof-of-concept. SMP has attracted the increasing interest of researchers, digital light processing (DLP) printing opens new opportunities to fabricated shape memory polymer, and it requests 3D-printable capability with more advanced shape-memory function and mechanical performance of material to broaden application of shape memory polymer.

Although people have been trying to improve the strain at break of epoxy based polymers [31, 32], the previously reported EAs still have a limited strain at break. Hence, in this work, a novel high strain EA-based SMP was fabricated by digital light processing (DLP) 3D printing. The liquid resin showed fast copolymerization of oligomers and monomers, which contributed to the ability to print a series of complex structures. The 3D-printed shape memory polymer showed superior and adjustable mechanical properties, thermal stability, as well as excellent shape memory performance. As a proof-of-concept, shape memory-based self-driven electronics was fabricated by combining shape memory polymer with light-absorbing and conductive ink. The device could change its configuration in response to light, indicating shape memory-based self-driven electronics has great potential application for soft robotics, flexible electronics, and intelligent control devices.

2. Materials and methods

2.1. Materials

Epoxy acrylate (EA) with two functional degrees was purchased from Guangzhou Runao Chemical Co. Ltd. Ltd. 2-Hydroxyethyl methacrylate (HEMA) was purchased from Chengdu Sicheng Photoelectric Material Co., Ltd. Tripropylene glycol diacrylate (TPGDA) was purchased from Shanghai Curease Chemical Co.Phenyl bis(2,4,6-trimethylbenzoyl)-phosphine oxide (Photoinitiator-819) was used as photoinitiator to initiate fast copolymerization of EA, HEMA and TPGDA at the wavelength of 405 nm. All materials used here were used as received without further purification.

2.2. 3D printing processing

The materials of liquid resin for 3D printing were prepared by mixing the EA, HEMA,TPGDA, as well as photoinitiator-819 with different weight ratios, EA as oligomer was applied as the base material of liquid resin because of its mechanical properties such as high toughness and stiffness [4]. In addition, HEMA and TPGDA were used as monomers of liquid resin. The mixture was stirred for 20 min at a temperature of 40 °C; the mixture was degassed in a vacuum oven and in the dark for 10 min for following 3D printing. In the current work, three different samples with different proportions were selected for analysis, as shown in Table 1.

A DLP-based 3D printer (Photon-s, Anycubic) which utilized a UV light source array with wavelength of 405 nm was used for 3D printing. The 405 nm of light from UV light source array was irradiated to liquid resin through transparent areas modified by LCD screen and solidified the liquid resin to form a patterned layer. The transparent released film was further used to ensure transmission of light and separated solid layer from liquid resin container. The linear motor with a platform was built for the printing of the photocurable liquid resin. The platform with

Table 1. The materials of liquid resin for 3D printing.

Samples	EA [g]	HEMA [g]	TPGDA [g]	Photoinitiator-819 [g]
SMP-1	5	15	2	0.6
SMP-2	10	10	2	0.6
SMP-3	15	5	2	0.6

solid structure was lifted, followed by subsequent irradiation and solidification steps until the whole 3D structure was fabricated. During the printing, the layer printing time was 30 s, and layer thickness was 50 μm (more details in Section 3.1).

2.3. Testing and characterization

The tensile tests were conducted by a mechanical testing machine (ZQ-990A, 200 N force sensor, China) at a rate of 1 mm·min^{-1}. The tensile stress and tensile strain were determined by the rupture point of the stress-strain curve, and the tensile tests were carried out at room temperature. The toughness was calculated from the area of stress-strain curves, and the elastic modulus was obtained from the linear region of the stress-strain curve. The Fourier Transform Infrared Reflection (FTIR) spectrum of shape memory polymer was acquired on an FTIR spectrometer (Nicolet 5700, China) from 4000 to 500 cm^{-1} with a 0.4 cm^{-1} resolution. The Thermo Gravimetry and Differential Scanning Calorimetry (TG-DSC) curves were performed on differential scanning calorimetry analysis (TA Q600, USA) at a heating rate of 10 °C/min in nitrogen atmosphere. The fold-deploy test was used to measure the fixity ratio (R_f) and shape recovery ratio (R_r); the angle was measured by an electronic digital angle ruler (details in Section 3.5). An infrared camera (FOTRIC-227S, China) was used to measure the distribution of temperature of the designed device irradiated by infrared light with the wavelength of 808 nm.

3. Results and discussion

3.1. Fabrication of SMP

The SMP was fabricated by down-top digital light processing (DLP) based on 3D printing (Figure 1a). The 3D models of physical parts were prepared on Solidworks, and the sliced digital images for the printer were generated by an open-source software-CHITUBOX. The sliced digital images were transported to liquid crystal display (LCD) with high resolution below 50 μm. The printed structure was put into ethanol and then washed with Ultrasonic Clear to remove the uncured liquid resin.

The chemical structures of liquid resin for 3D printing were shown in Figure 1b, EA acts as an oligomer, TPGDA and HEMA are the monomers. In addition, the 819 acts as a photoinitiator to initiate copolymerization of the oligomer and monomers at the wavelength of 405 nm, which solidifies the liquid resin to

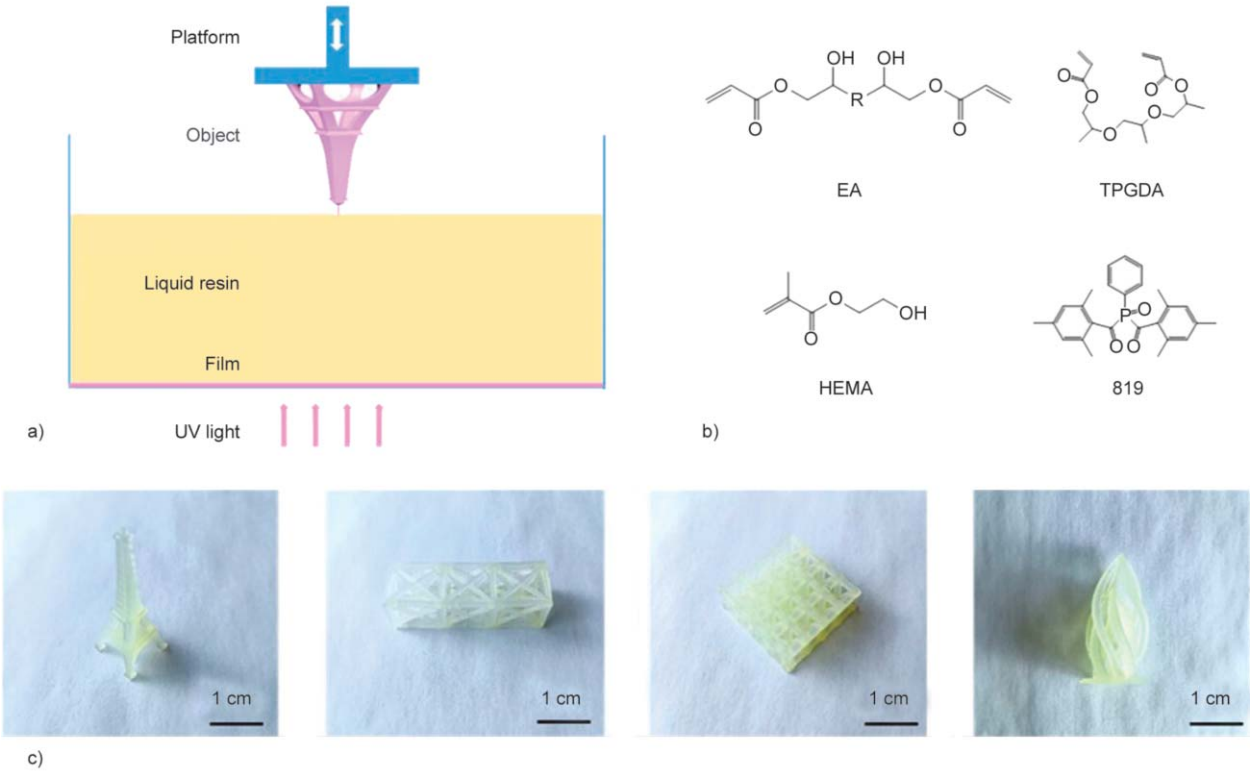

Figure 1. Fabrication and materials of shape memory polymer. (a) 3D printing procedures and schematic diagrams of DLP-based 3D printing technology. (b) Materials and chemical structures of liquid resin for 3D printing. (c) Structures fabricated by 3D printing.

form a solid structure. Using the 3D printing technology and liquid resin, we fabricated a series of complex structures, including the Eiffel tower and other lattice array structures.

3.2. FTIR analysis of SMP

The FTIR spectrum of 3D-printed SMPs with different content of monomers is shown in Figure 2. The strong peak around 1725 cm^{-1} was ascribed to the stretching vibration of C=O, the peak at 2927 cm^{-1} was assigned to the stretching vibration of –CH3, and the characteristic peak at 2872 cm^{-1} was due to the stretching vibration of $–CH_2$. In addition, the strong peak at 3436 cm^{-1} was ascribed to the stretching vibration of O–H, and it could be seen that the intensity of peaks around 1725 and 3436 cm^{-1} attenuated with the increase of monomers content.

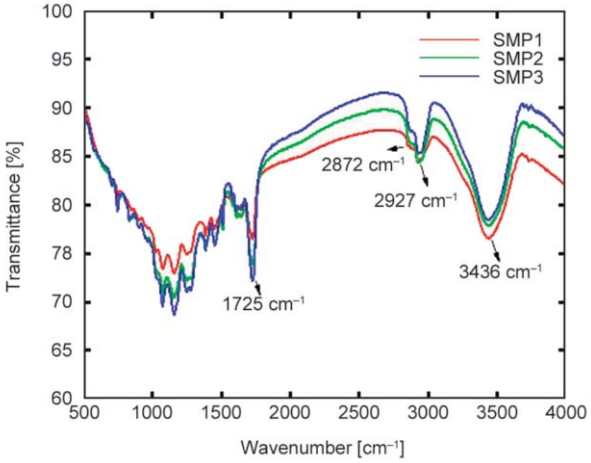

Figure 2. FTIR spectrum of 3D-printed SMPs with different content of monomers.

3.3. Mechanical performance of SMP

The mechanical properties of SMPs were investigated. The typical stress-strain curves of shape memory polymers with different contents of the oligomer and monomers were shown in Figure 3a. EA worked as the oligomer, TPGDA and HEMA worked as the monomers. With the addition of monomers, the tensile strength of the SMP increased, and the elongation at break decreased gradually. Figure 3b shows the details of tensile properties with different ratios of the oligomer to monomers. With the addition of monomers, the elongation of SMP at break decreased from 90.16to 52.94%, and the elastic modulus of SMP increased from 12.26 to 107.98 MPa. This is due to the addition of monomers as 'hard segments' to SMP could significantly enhance the entanglement of the molecular chain, which could increase the tensile stress and elastic modulus. However, the addition of epoxy acrylate as the 'soft segment' could weaken the entanglement of the molecular chain, resulting in a decrease in tensile strength but an increase in elongation at break. Toughness is a significant factor in characterizing the mechanical properties of SMP. As shown in Figure 3b, the toughness of SMP relied on the amount of monomer; the toughness increased from 2.70 to 6.34 MPa with the addition of monomer. The results from uniaxial tensile tests demonstrated the high strain and toughness of 3D-printed SMP.

3.4. Thermal performance of SMP

The thermal stability of the shape memory polymer was first investigated by TG tests. The TG curves of

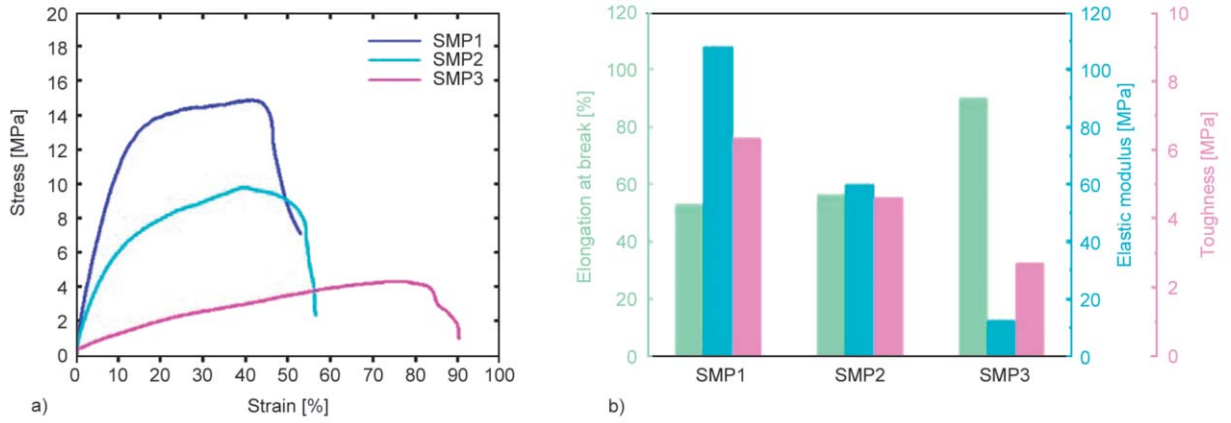

Figure 3. The mechanical properties of SMPs. (a) Uniaxial tensile tests of SMPs with different content of the oligomer and monomers. (b) The calculated elongation at break, elastic modulus, and toughness of SMPs with various contents of the oligomer and monomers.

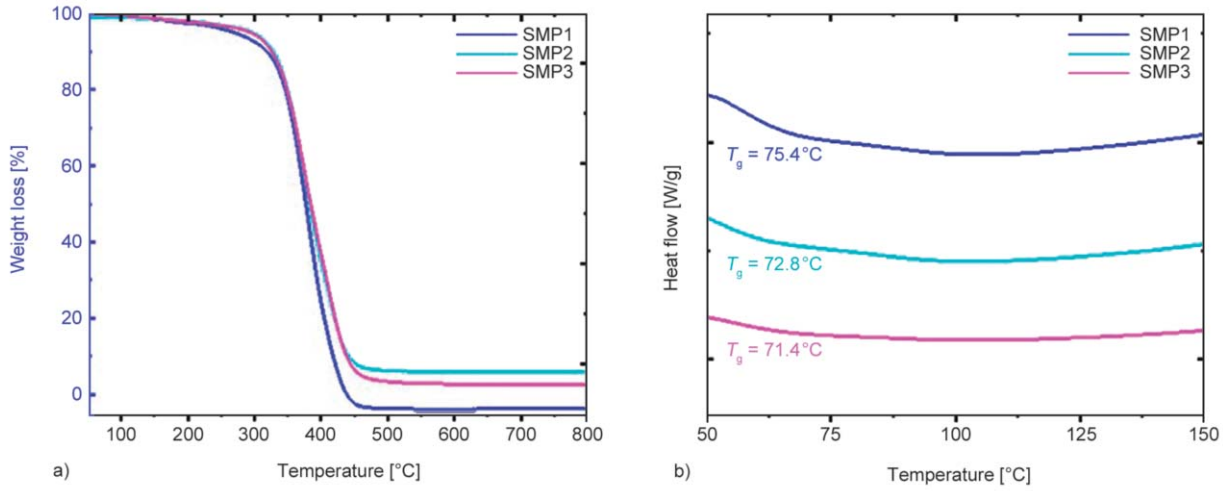

Figure 4. TG-DSC analysis of 3D-printed SMPs. (a) The TG curves of SMPs with different content of monomers. (b) DSC curves of SMPs with different monomer contents.

SMP with different content of monomers were shown in Figure 4a. The weight loss curves (Figure 4a) revealed that the initial degradation temperature of SMP with low monomer content was significantly higher than that of the others. In other words, degradation temperature could be significantly improved by the addition of epoxy acrylate. The DSC curve used to determine the effect of monomer content on the glass transition temperature (T_g) of SMP is shown in Figure 4b. As can be seen from the curve, with the addition of monomers, the glass transition temperature (T_g) increased from 71.7 to 75.4 °C. Moreover, with an increase of the toughness of the EA-based SMP, the T_g increases. The temperature above the glass transition temperature (T_g) of SMP was used as the programmed temperature to actuate the shape memory property in the subsequent experiments [5].

3.5. Shape memory properties of SMP

A fold-deploy test was applied to demonstrate the shape memory performance of 3D- printed SMP. Figure 5a shows the schematic diagrams of the shape memory process. Considering both toughness and elongation, here, SMP2 based sample was used to investigate the shape memory. The fold-deploy test was carried out as follows: Firstly, a 3D printed sample ($\theta_0 = 0°$) was heated to 80 °C (above the glass transition temperature (T_g) of SMP) for 30s, then, the printed sample was bent into 'U' shape from the center axis with external force ($\theta_u = 180°$). Secondly, the deformed 'U' shape was cooled down to 20 °C (room temperature) and removed the external force to fix its shape, which acts as a temporary shape (θ_f). Then, the temporary shape was reheated to 80 °C (above the glass transition temperature (T_g) of SMP) to recover to its original shape, and the angle was measured as recovery angle (θ_r). The shape fixity ratio (R_f) and shape recovery ratio (R_r) were calculated by Equations (1) and (2), as reported previously [33]:

$$R_f = \frac{\theta_u - \theta_f}{\theta_u} \cdot 100\% \quad (1)$$

$$R_r = \frac{\theta_u - \theta_r}{\theta_u - \theta_0} \cdot 100\% \quad (2)$$

As shown in Figure 5b, the temporary shape could recover its original 3D-printed shape within 30 s, and the samples recover faster at a higher temperature, which is mainly attributed to the higher mobility of polymer chain segments at a higher temperature. The results show excellent shape memory performance, including high recovery angle and high recovery speed. In addition, the value of shape fixity ratio (R_f) and shape recovery ratio (R_r) during 5 cycles at the temperature of 80 °C was determined (Figure 5c), It could be seen that the average shape fixity ratio (R_f) and shape recovery ratio (R_r) were 98.5, 98.4%, respectively, indicating the stability of shape memory effect.

We further fabricated a series of shape memory complex structures by DLP-based 3D printing technology. Figure 6 shows the shape memory process of printed structures that are a challenge to fabricate by traditional manufacturing approaches. The printed shape was easily programmed to temporary and could recover to its original shape; it can be seen that the recovered shape was almost exactly the same as

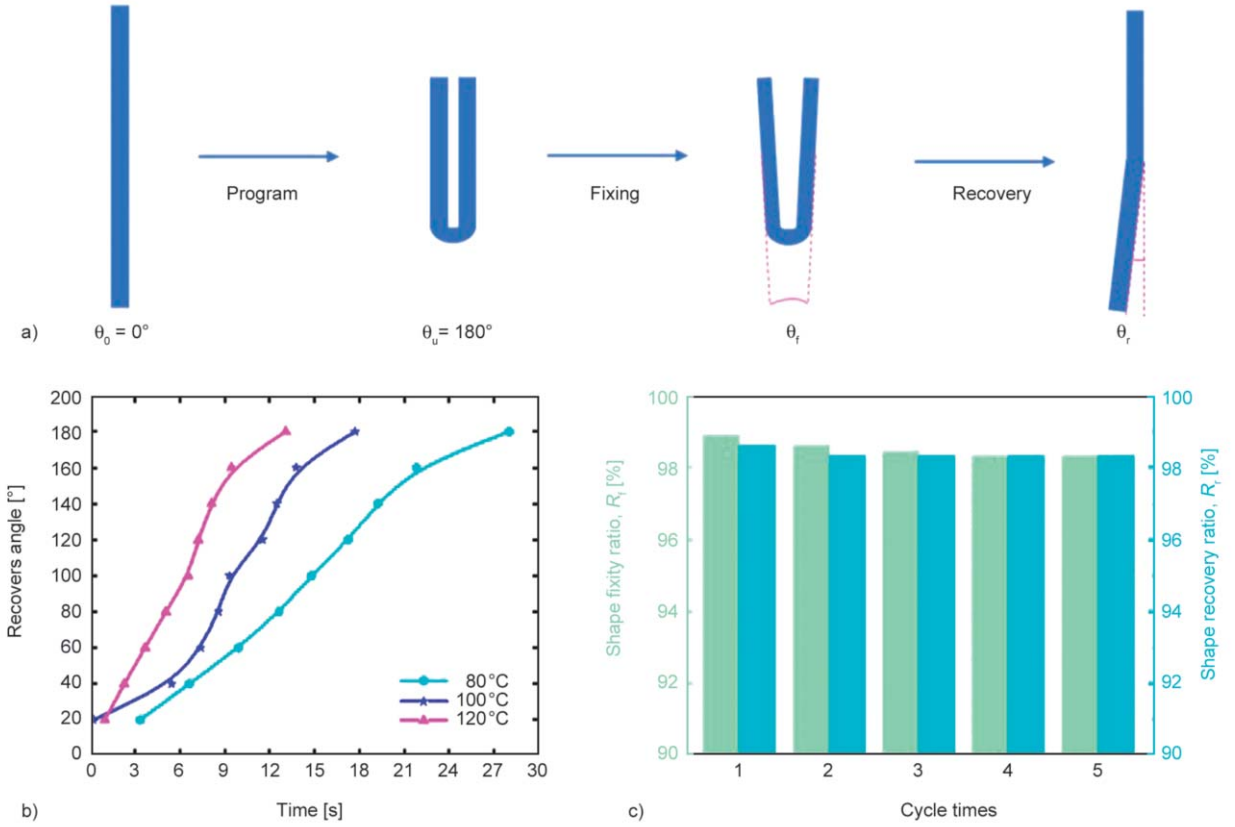

Figure 5. Shape memory properties of 3D-printed SMP. (a) Schematic diagrams of the shape memory process. (b) Recovery angle with time at different temperatures. (c) Shape fixity and the recovery ratio of SMP.

Figure 6. Shape memory process of complex structures fabricated by DLP-based 3D printing technology.

the 3D-printed original shape, indicating that shape memory behavior with a complex structure that could be used applied in the field of actuators, soft robotics, as well as aerospace.

3.6. Self-driven electronics by SMP

The 3D-printed shape-memory structures can be applied in light-operated smart devices by integrating the SMP with conductive and light-absorbing materials, and we demonstrate possible applications in shape memory-based self-driven electronics. This device consisted of an SMP with light-absorbing and conductive ink. The ink was prepared by mixing the activated carbon, acetylene black, and PTFE with a weight ratio of 8:1:1, and the mixture was dispersed in ethanol to form a slurry. Then, this slurry was uniformly coated onto a 3D-printed SMP. Finally, two individual copper ribbons were attached to both sides of 3D-printed SMP to obtain shape memory-based self-driven electronics. The device was dried for 30 min for the ethanol to evaporate. As shown in Figure 7a, the temporary shape of shape memory-based self-driven electronics was a closed electrical circuit, which could act as a conductor to light the LED bulb, when the shape memory-based self-driven electronics was irradiated by infrared light with the wavelength of 808 nm, the infrared light modulated the temperature exceed the glass transition temperature (T_g), enables the SMP to recover to its original shape, resulting in an open electrical circuit with LED bulb off (Figure 7b, 7c). Moreover, the images taken by the infrared camera also clearly show light-operated temperature exceed glass transition temperature (T_g) to complete the shape memory process (Figure 7d). The results indicate shape memory-based self-driven electronics has great potential application for soft robotics, flexible electronics, and intelligent control devices.

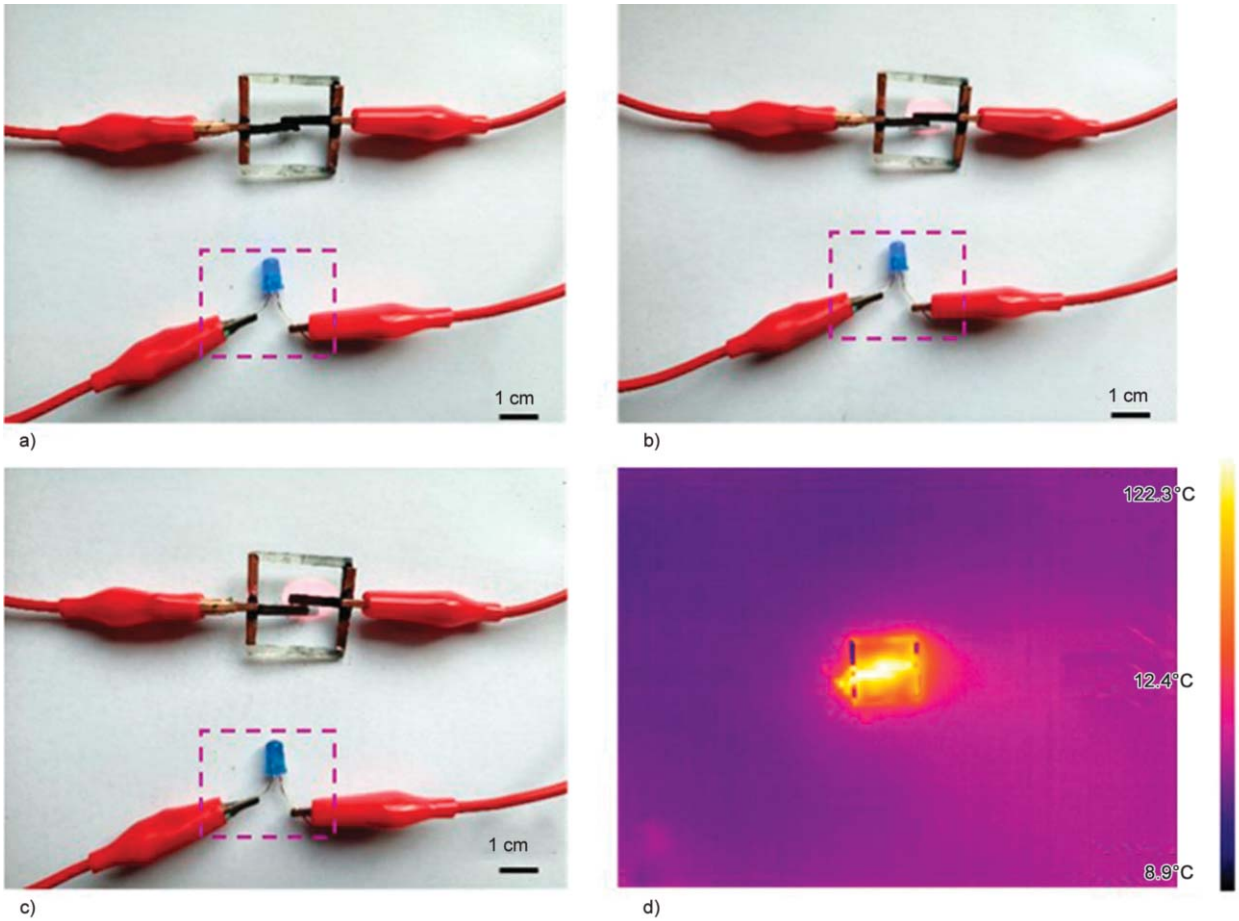

Figure 7. Light-operated smart device fabricated by SMP. (a) The temporary shape of shape memory-based self-driven electronics with a closed electrical circuit. (b) Shape memory-based self-driven electronics was irradiated by infrared light with a wavelength of 808 nm. (c) The recovered shape of shape memory-based self-driven electronics with an open electrical circuit. (d) Distribution of temperature of designed device irradiated by infrared light with the wavelength of 808 nm.

4. Conclusions

In summary, we developed the outlined new strategy for fabrication of shape memory through digital light processing (DLP). 3D-printing took advantage of free-radical copolymerization of EA-based oligomers and monomers. The uniaxial tensile tests demonstrated the 3D-printed EA-based SMP with a high strain (up to 90%) and toughness. TG-DSC analysis showed that SMP has excellent thermal stability. Fold-deploy experiments were applied to evaluate the SMP with outstanding shape memory performance, including a high shape fixity ratio (R_f) of 98.5%, shape recovery ratio (R_r) of 98.4%, and high recovery speed (12 s). With the advantages of easy fabrication, mechanical properties, as well as outstanding shape memory performance, the shape memory-based self-driven electronics was fabricated by combining SMP with light-absorbing and conductive ink. The device could change its configuration in response to light, which has great potential application for soft robotics, flexible electronics, and intelligent control devices.

Acknowledgements

This work was supported by Natural Science Foundation of Hunan Province (2019JJ50063)

References

[1] He Z., Satarkar N., Xie T., Cheng Y-T., Hilt J. Z.: Remote controlled multishape polymer nanocomposites with selective radiofrequency actuations. Advanced Materials, **23**, 3192–3196 (2011). https://doi.org/10.1002/adma.201100646

[2] Li J., Duan Q., Zhang E., Wang J.: Applications of shape memory polymers in kinetic buildings. Advances in Materials Science and Engineering, **2018**, 7453698/1–7453698/13 (2018). https://doi.org/10.1155/2018/7453698

[3] Kardar P., Ebrahimi M., Bastani S., Jalili M.: Using mixture experimental design to study the effect of multifunctional acrylate monomers on UV cured epoxy acrylate resins. Progress in Organic Coatings, **64**, 74–80 (2009). https://doi.org/10.1016/j.porgcoat.2008.07.022

[4] Chen K., Kuang X., Li V., Kang G., Qi H. J.: Fabrication of tough epoxy with shape memory effects by UV-assisted direct-ink write printing. Soft Matter, **14**, 1879–1886 (2018). https://doi.org/10.1039/C7SM02362F

[5] Yu R., Yang X., Zhang Y., Zhao X., Wu X., Zhao T., Zhao Y., Huang W.: Three-dimensional printing of shape memory composites with epoxy-acrylate hybrid photopolymer. ACS Applied Materials and Interfaces, **9**, 1820–1829 (2017). https://doi.org/10.1021/acsami.6b13531

[6] Shan W., Chen Y., Hu M., Qin S., Liu P.: 4D printing of shape memory polymer *via* liquid crystal display (LCD) stereolithographic 3D printing. Materials Research Express, **7**, 105305/1–105305/12 (2020). https://doi.org/10.1088/2053-1591/abbd05

[7] Ambrosi A., Pumera M.: 3D-printing technologies for electrochemical applications. Chemical Society Reviews, **45**, 2740–2755 (2016). https://doi.org/10.1039/C5CS00714C

[8] Ligon S. C., Liska R., Stampfl J., Gurr M., Mülhaupt R.: Polymers for 3D printing and customized additive manufacturing. Chemical Reviews, **117**, 10212–10290 (2017). https://doi.org/10.1021/acs.chemrev.7b00074

[9] Mohamed M. G. A., Kumar H., Wang Z., Martin N., Mills B., Kim K.: Rapid and inexpensive fabrication of multi-depth microfluidic device using high-resolution LCD stereolithographic 3D printing. Journal of Manufacturing and Materials Processing, **3**, 3010026/1–3010026/11 (2019). https://doi.org/10.3390/jmmp3010026

[10] Kang J., Shangguan H., Deng C., Hu Y., Yi J., Wang X., Zhang X., Huang T.: Additive manufacturing-driven mold design for castings. Additive Manufacturing, **22**, 472–478 (2018). https://doi.org/10.1016/j.addma.2018.04.037

[11] Xing J-F., Zheng M-L., Duan X-M.: Two-photon polymerization microfabrication of hydrogels: An advanced 3D printing technology for tissue engineering and drug delivery. Chemical Society Reviews, **44**, 5031–5039 (2015). https://doi.org/10.1039/C5CS00278H

[12] Noor N., Shapira A., Edri R., Gal I., Wertheim L., Dvir T.: 3D printing of personalized thick and perfusable cardiac patches and hearts. Advanced Science, **6**, 1900344/1–1900344/10 (2019). https://doi.org/10.1002/advs.201900344

[13] Lei Z., Wang Q., Wu P.: A multifunctional skin-like sensor based on a 3D printed thermo-responsive hydrogel. Materials Horizons, **4**, 694–700 (2017). https://doi.org/10.1039/c7mh00262a

[14] Wang Z., Gao W., Zhang Q., Zheng K., Xu J., Xu W., Shang E., Jiang J., Zhang J., Liu Y.: 3D-printed graphene/polydimethylsiloxane composites for stretchable and strain-insensitive temperature sensors. ACS Applied Materials and Interfaces, **11**, 1344–1352 (2019). https://doi.org/10.1021/acsami.8b16139

[15] Gong H., Beauchamp M., Perry S., Woolley A. T., Nordin G. P.: Optical approach to resin formulation for 3D printed microfluidics. RSC Advances, **5**, 106621–106632 (2015). https://doi.org/10.1039/C5RA23855B

[16] Gong H., Bickham B. P., Woolley A. T., Nordin G. P.: Custom 3D printer and resin for 18 μm × 20 μm microfluidic flow channels. Lab on a Chip, **17**, 2899–2909 (2017). https://doi.org/10.1039/C7LC00644F

[17] Layani M., Wang X., Magdassi S.: Novel materials for 3D printing by photopolymerization. Advanced Materials, **30**, 1706344/1–1706344/7 (2018). https://doi.org/10.1002/adma.201706344

[18] Zhang W., Wang H., Wang H., Chan J. Y. E., Liu H., Zhang B., Zhang Y-F., Agarwal K., Yang X., Ranganath A. S., Low H. Y., Ge Q., Yang J. K. W.: Structural multicolour invisible inks with submicron 4D printing of shape memory polymers. Nature Communications, **12**, 112/1–112/8 (2021). https://doi.org/10.1038/s41467-020-20300-2

[19] Odent J., Wallin T. J., Pan W., Kruemplestaedter K., Shepherd R. F., Giannelis E. P.: Highly elastic, transparent, and conductive 3D-printed ionic composite hydrogels. Advanced Functional Materials, **27**, 1701807/1–1701807/10 (2017). https://doi.org/10.1002/adfm.201701807

[20] Han D., Farino C., Yang C., Scott T., Browe D., Choi W., Freeman J. W., Lee H.: Soft robotic manipulation and locomotion with a 3D printed electroactive hydrogel. ACS Applied Materials and Interfaces, **10**, 17512–17518 (2018). https://doi.org/10.1021/acsami.8b04250

[21] Peng B., Yang Y., Gu K., Amis E. J., Cavicchi K. A.: Digital light processing 3D printing of triple shape memory polymer for sequential shape shifting. ACS Materials Letters, **1**, 410–417 (2019). https://doi.org/10.1021/acsmaterialslett.9b00262

[22] Zarek M., Layani M., Cooperstein I., Sachyani E., Cohn D., Magdassi S.: 3D printing of shape memory polymers for flexible electronic devices. Advanced Materials, **28**, 4449–4454 (2016). https://doi.org/10.1002/adma.201503132

[23] Zhao T., Yu R., Li X., Cheng B., Zhang Y., Yang X., Zhao X., Zhao Y., Huang W.: 4D printing of shape memory polyurethane *via* stereolithography. European Polymer Journal, **101**, 120–126 (2018). https://doi.org/10.1016/j.eurpolymj.2018.02.021

[24] Deng Y., Li J., He Z., Hong J., Bao J.: Urethane acrylate-based photosensitive resin for three-dimensional printing of stereolithographic elastomer. Journal of Applied Polymer Science, **137**, 49294/1–49294/12 (2020). https://doi.org/10.1002/app.49294

[25] Peng S., Li Y., Wu L., Zhong J., Weng Z., Zheng L., Yang Z., Miao J-T.: 3D printing mechanically robust and transparent polyurethane elastomers for stretchable electronic sensors. ACS Applied Materials and Interfaces, **12**, 6479–6488 (2020). https://doi.org/10.1021/acsami.9b20631

[26] Zolfagharian A., Kouzani A. Z., Khoo S. Y., Moghadam A. A. A., Gibson I., Kaynak A.: Evolution of 3D printed soft actuators. Sensors and Actuators A: Physical, **250**, 258–272 (2016). https://doi.org/10.1016/j.sna.2016.09.028

[27] Invernizzi M., Turri S., Levi M., Suriano R.: 4D printed thermally activated self-healing and shape memory polycaprolactone-based polymers. European Polymer Journal, **101**, 169–176 (2018). https://doi.org/10.1016/j.eurpolymj.2018.02.023

[28] Han D., Lu Z., Chester S. A., Lee H.: Micro 3D printing of a temperature-responsive hydrogel using projection micro-stereolithography. Science Report, **8**, 1963/1–1963/10 (2018). https://doi.org/10.1038/s41598-018-20385-2

[29] Zhao T., Yu R., Li S., Li X., Zhang Y., Yang X., Zhao X., Wang C., Liu Z., Dou R., Huang W.: Superstretchable and processable silicone elastomers by digital light processing 3D printing. ACS Applied Materials and Interfaces, **11**, 14391–14398 (2019). https://doi.org/10.1021/acsami.9b03156

[30] Wang J., Xue Z., Li G., Wang Y., Fu X., Zhong W-H., Yang X.: A UV-curable epoxy with 'soft' segments for 3D-printable shape-memory materials. Journal of Materials Science, **53**, 12650–12661 (2018). https://doi.org/10.1007/s10853-018-2520-0

[31] Zheng N., Fang G., Cao Z., Zhao Q., Xie T.: High strain epoxy shape memory polymer. Polymer Chemistry, **6**, 3046–3053 (2015). https://doi.org/10.1039/C5PY00172B

[32] Dhulst E. A., Heath W. H., Torkelson J. M.: Hybrid thiol-acrylate-epoxy polymer networks: Comparison of one-pot synthesis with sequential reactions and shape memory properties. Polymer, **96**, 198–204 (2016). https://doi.org/10.1016/j.polymer.2016.04.032

[33] Zhang R., Wang S., Tian J., Chen K., Xue P., Wu Y., Chou W.: Effect of PEW and CS on the thermal, mechanical, and shape memory properties of UHMWPE. Polymers, **12**, 12020483/1–12020483/15 (2020). https://doi.org/10.3390/polym12020483